Petroleum and Coal

Article **Open Access**

Reservoirs Stability Evaluation through Analysis of Rock Mechanical Parameters and Stresses in "Beta" Field, Offshore Niger Delta, Nigeria

C. C. Agoha[1], A. I. Opara[1], O. C. Okeke[1], C. N. Okereke[1], C. C. Z. Akaolisa[1], C. N. Onwubuariri[2], I. A. Omenikolo[3] and C. B. Agbakwuru[3]*

[1] Department of Geology, Federal University of Technology, P.M.B. 1526, Owerri, Imo State, Nigeria
[2] Department of Physics, Michael Okpara University of Agriculture Umudike, Abia State, Nigeria
[3] Department of Physics, Federal Polytechnic Nekede, Owerri, Imo State, Nigeria

Received February 21, 2023; Accepted July 3, 2023

Abstract

The geomechanical characterization of the reservoirs of "Beta Field" was carried out to predict the stability of hydrocarbon reservoir rocks and hence, mitigate drilling and exploitation challenges within offshore Niger Delta. Gamma ray, sonic, and density logs from four wells within the field, including core data and 3D reflection seismic volume from the area, were integrated to determine rock mechanical and petrophysical properties from empirical equations, and generate 3D geomechanical models using Petrel and Ms-Excel software. Principal stresses operating within the reservoirs and pore pressure were also estimated from empirical models. Cross plots of these rock parameters were obtained to ascertain the relationship between them and obtain model equations. Results show that the rock mechanical properties have lower values in sand units than shale units with petrophysical parameters having lower values in shale. Average values of 13.70GPa, 0.33, 13.30GPa, 32.32GPa, 5.12GPa, 0.07, and 0.022mD were obtained in shale; while 0.30, 10.94GPa, 0.30, 12.76GPa, 25.19GPa, 4.11GPa, 0.19, and 192.00mD were recorded in sand for Young's modulus, Poisson ratio, bulk modulus, uniaxial compressive strength, shear modulus, effective porosity, and permeability respectively. Mean pore pressures observed in sand and shale units are 13,683psi and 15,662psi while mean total vertical stress, maximum and minimum horizontal stresses recorded in the reservoirs are 28,392psi, 25,537psi and 20,781psi respectively. Comparative analysis of obtained rock mechanical and strength parameters with the principal stresses operating within the reservoirs show that the studied reservoirs and by extension reservoirs of this petroleum play are stable.

Keywords*: Geomechanical model; Petrophysical properties; Principal stresses; Empirical equations; Pore pressure; Petroleum play.*

1. Introduction

The study of the mechanical behavior of rocks under different stress or pressure conditions is referred to as geomechanics. It studies the mechanical response of rocks to the events that disturb their initial state [1]. Geomechanics play a very vital role in assessing formation integrity during well construction and completion and in the response of the reservoir to oil production, hydraulic fracturing, and depletion [2]. It is used to reduce risks and optimize rewards related to the mechanical failure of the reservoir and surrounding formations resulting from hydrocarbon exploration and production activities [3]. In fact, the aim of analyzing wellbore stability is to reduce the myriad of challenges associated with drilling operations [4].

The past two decades have seen the science of geomechanics widen its territory of practice from smallscale analysis of boreholes to large scale reservoir study due to hydrocarbon search in unconventional plays, increasing awareness of the concept of caprock integrity and reservoir containment, increasing number of subsurface waste storage projects [1]. Geophysics in reservoir exploration and exploitation has evolved in role with rock mechanics assuming center stage in energy resources development and sustainability [5]. This can be attributed to the array of problems encountered by operators during the life cycle of hydrocarbon reservoirs and at every stage of their well life. This is especially in unconventional plays like the offshore Niger Delta basin which comprises deep water, high temperature, high pressure, and complexly faulted reservoirs that are usually characterized by increased stress changes and reduced permeability during production. With the increasing requirement for hydrocarbon exploration and development in deep water, unconventional and other challenging environments, accurate geomechanical modeling and characterization have become ever more critical in ensuring safe and cost-effective operations [6].

Previous authors including [6-11] have studied the geomechanical characteristics of different rock formations in different geological provinces, ranging from reservoir geomechanical studies to caprock integrity and wellbore stability, to obtain accurate geomechanical characterizations of the rocks of those areas. [12] and [13] have also carried out studies on the principal stresses operating within parts of the onshore Niger Delta and the geomechanical characterization and modeling of hydrocarbon reservoirs in parts of the Niger Delta to determine the nature and strength of reservoirs in parts of the Delta. It is, however, observed that most of these studies are onshore Niger Delta, and only 1D or 2D geomechanical models were employed for investigation. Few of the studies employing 3D geomechanical models did not integrate core data. This work, which is offshore Niger Delta, therefore has the advantage of integrating well log information, core data, and 3D seismic volume from the study field. This unique data combination guaranteed the reliability of interpreted results and revealed much more detailed geomechanical information about the reservoirs of the fields under investigation. This study also generated and validated novel model mathematical equations which can be applied in determining rock uniaxial compressive strength from any of Young's modulus, effective porosity, shear modulus, and measured depth.

The objectives of the present study are to determine rock elastic properties of bulk modulus, Poisson ratio, shear modulus, Young's modulus, and bulk compressibility of the reservoirs; to determine rock inelastic property of unconfined or uniaxial compressive strength of the reservoir; to determine the petrophysical properties of the reservoirs including permeability, effective porosity, and total porosity; and generate reservoir 3D geomechanical models using sonic, density, and gamma ray logs in addition to core information and seismic 3D volume from the field. The relationship between rock inelastic, elastic, and petrophysical properties was investigated to ascertain their interrelationship. Model equations were also obtained from these relationships and validated. Figure 1 is an illustration of the stresses and resultant deformation in a reservoir and its surroundings.

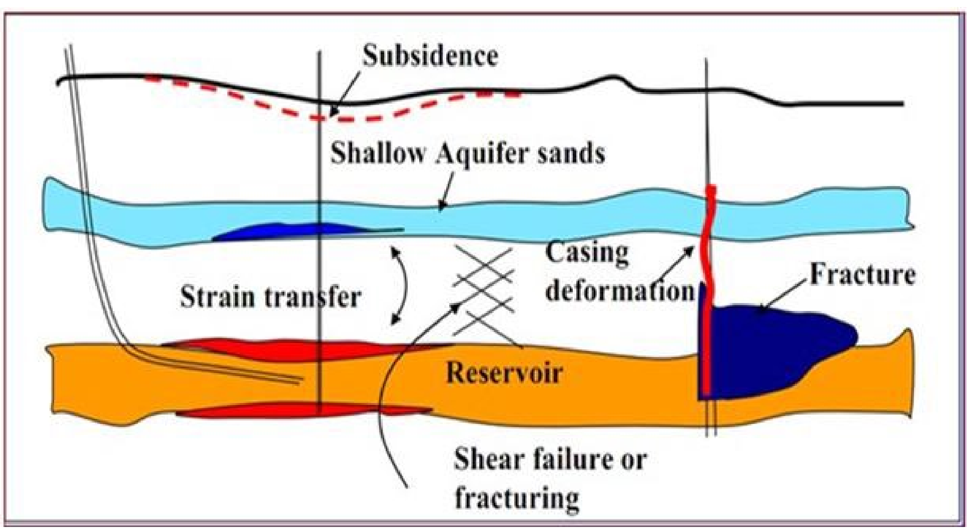

Figure 1. Diagram showing the stresses and resultant deformation in the reservoir and its surroundings (source: [14])

2. Location and background geology of the area

The study location is an offshore oil field situated within the eastern axis of the offshore depobelt, one of the depobelts within the basin of the Niger Delta. Beta Field is situated within latitudes 3°56'35.715"N and 4°03'7.466"N, and longitudes 6°25'25.971"E and 6°32'10.372"E. Figure 2 shows the license map of parts of Niger Delta basin indicating Beta Field location.

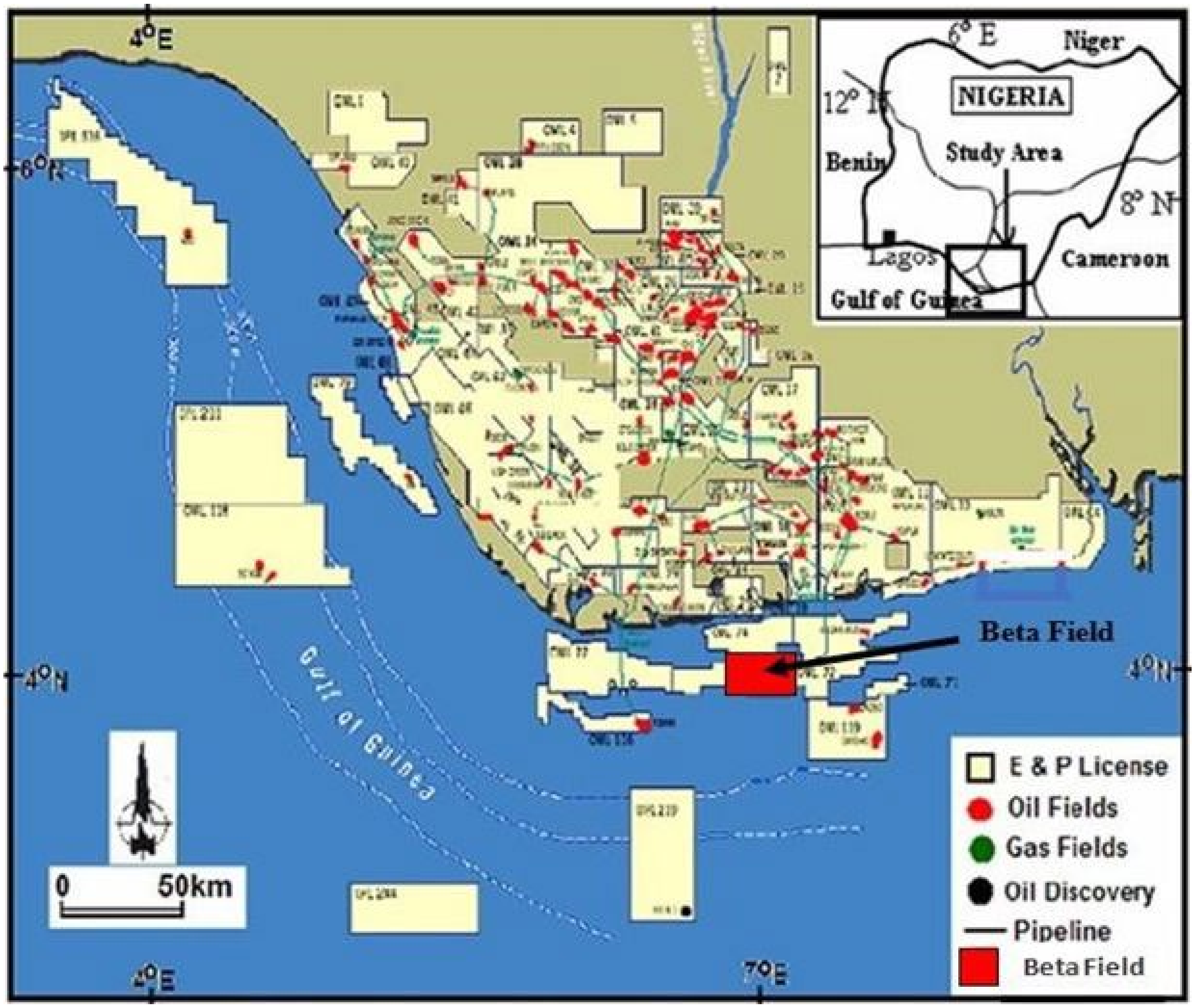

Figure 2.License map of parts of the Niger Delta basin indicating the study field location (modified from [15])

The Niger delta is a basin that is located on the continental margin of West Africa, at the top of the Gulf of Guinea where the site of a triple junction was formed during Cretaceous continental break-up. The area of this delta is about 200,000 square kilometers [16].

The delta is made up of three generalized lithostratigraphic units namely (from oldest to youngest) Akata, Agbada, and the topmost Benin Formations [17]. The Akata Formation is the basal unit consisting of massive monotonous and generally dark grey marine shales. The formation is generally very rich in fauna and flora remains [16]. Sandstone lenses (rings) called turbidites occur near the top of the formation, particularly at the contact with the overlying Agbada Formation. Akata Formation is the major source rock for the hydrocarbons of the Niger delta [18]. Its thickness is uncertain but may reach 7000m in the central part of the delta with age ranging from Paleocene to Holocene [19]. The Agbada formation overlies the Akata (basal) Formation and it is a paralic sequence represented by an alternation of sandstones and shales in various proportions [16]. This Formation forms the hydrocarbon prospective sequence (reservoir) in the Niger Delta and most exploration wells are located in this Formation [16]. The sandstones constitute the main hydrocarbon reservoirs and the shales constitute the cap rocks or seals [20]. The age of the formation varies from Pleistocene around the southern axis to Eocene around the north and Recent at the delta surface. The youngest and the shallowest part of the Niger delta's lithostratigraphic units is the Benin Formation. It is composed almost entirely of non-marine sands and gravels. The formation has high sand content (over 90%) and little shale. The sands have shale intercalations that become more abundant towards their base [15]. To date, only oil shows have been found associated with this highly porous and generally fresh water-bearing sand formation [17,21]. The formation reaches a maximum thickness of 2,100m in the central Niger delta where there is maximum subsidence of the basement [18]. The age ranges from Oligocene in the north to Recent in the distal part of the Niger delta. Figure 3 shows the regional geological map of the Niger Delta culled from [22].

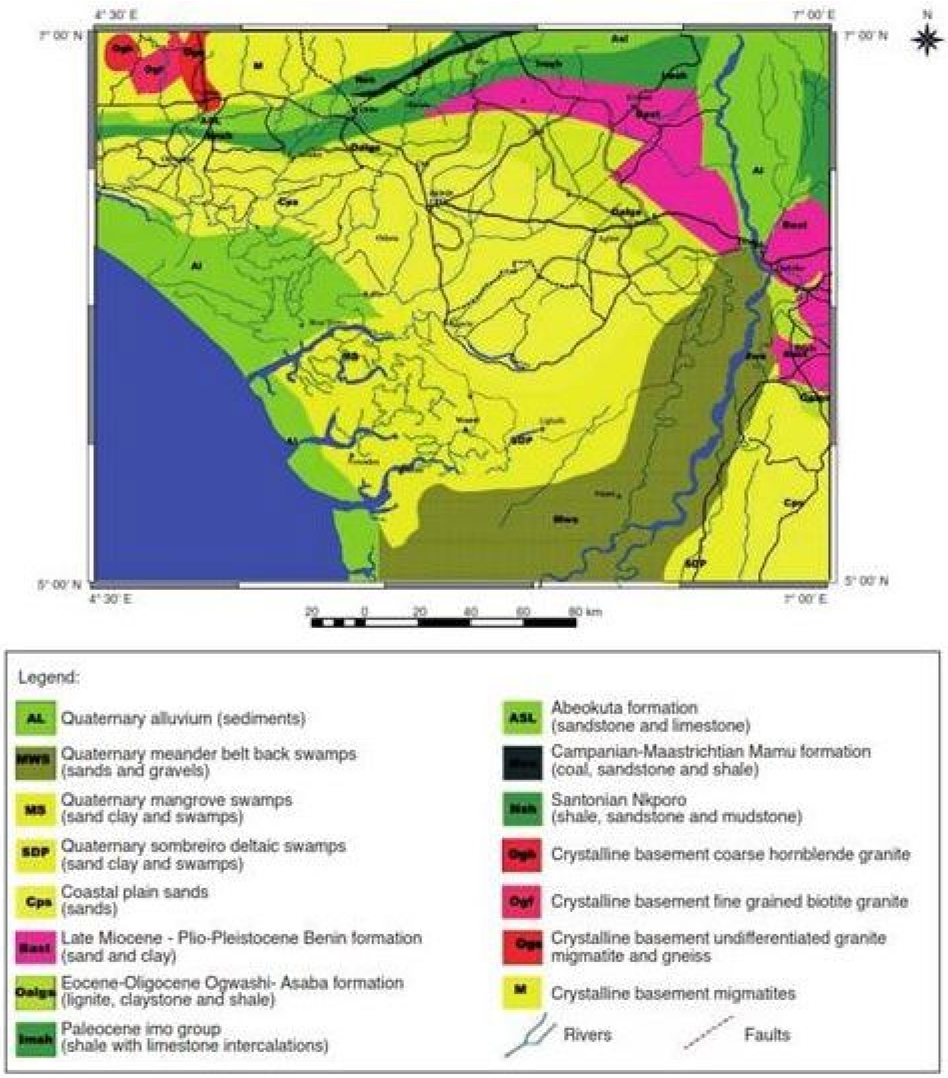

Figure 3. Regional geological map of the Niger Delta Basin, Nigeria (after [22])

3. Materials and methods

3.1. Data

The data employed in carrying out this study includes 3D reflection seismic volume acquired over the field; log suites comprising gamma ray log, sonic log, and bulk density log from four different wells within the field; core data from the four different wells; check-shot data for the field; well reports from the study field; and base map for the field.

The hardware and software employed in processing and analyzing the various dataset for this study include a standard workstation, Petrel to simulation software, and Microsoft Excel software.

3.2. Methods

The initial steps involved importing the different datasets into Petrel and Microsoft Excel software and saving them in text-delimited format. The datasets were quality-checked for possible errors. To identify the shale units and sand units within the study reservoir, stratigraphic correlation was carried out with the aid of well-log data. This was done since different sonic transit times, different density information, and in some cases, different empirical formulas are applied for sand and shale. The four wells were correlated to achieve this. The well-to-seismic tie was then carried out to ensure that the well logs and the seismic data are in agreement. This was followed by horizon and fault picking. Through identification of important surfaces, which are of interest, from the study Wells on a panel used for correlation of Wells, reservoir structure delineation was done using seismic data and well log information.

Dynamic elastic and inelastic as well as petrophysical properties of the reservoirs were then calculated using empirical relationships. The elastic rock parameters determined include Poisson ratio (*σ*), shear or rigidity modulus (μ), bulk modulus (*K*), bulk compressibility (C_b), and Young's modulus (*E*) while the inelastic rock property determined in this study is the uniaxial compressive strength (*UCS*) of the reservoirs. Petrophysical rock parameters including effective porosity ($Ø_{eff}$), permeability (*k)*, and total porosity ($Ø_T$), were obtained also using suitable empirical equations. The following empirical equations were employed in calculating rock mechanical and petrophysical parameters.

Poisson's ratio (σ) was obtained from equation (1) by [23] given by

$$\sigma = \frac{0.5(V_P^2 - 2V_S^2)}{(V_P^2 - V_S^2)} \tag{1}$$

where V_p is the compressional or primary wave velocity and V_s is the shear or secondary wave velocity.

Compressional wave velocity (V_p) was calculated from sonic data using the following relationship (equation 2):

$$V_P = \frac{304878}{Sonic/1000} \text{in km/s} \tag{2}$$

Computation of shear wave velocity (V_s) was from compressional wave velocity (V_p) using the [24] velocities for sand and shale beds given by equations 3 and 4 as:

$$V_s = 0.80416V_p - 0.85588 \text{ (for sand beds)} \tag{3}$$

$$V_s = 0.76969V_p - 0.86735 \text{ (for shale beds)} \tag{4}$$

Shear modulus (μ) was estimated from equation 5 given by:

$$\mu = \frac{a\rho_b}{V(\Delta Ts)} \tag{5}$$

where ρ_b is formation bulk density estimated from well log data; a is a coefficient which equals 13464; and ΔT_s is the change in shear sonic transit time obtained from the reciprocal of shear wave velocity (V_s) given by equation 6 as:

$$T_s = 1/V_s \tag{6}$$

Bulk modulus (K) was calculated from equation 7 expressed as:

$$K = a\rho_b\left[\frac{1}{\Delta T_C^2} - \frac{4}{3T_S^2}\right] \tag{7}$$

where ΔT_c represents sonic transit time (compressional) obtained from reciprocal of compressional wave velocity (V_p) given by equation 8 as:

$$T_c = 1/V_p \tag{8}$$

Bulk compressibility (C_b) was estimated from the inverse of bulk modulus given by equation 9 as:

$$C_b = 1/K = \frac{3\Delta T_C^2 T_S^2}{a\rho_b[3T_S^2 - 4T_C^2]} \tag{9}$$

Young's modulus (E) was calculated from equation 10 relating Young's modulus (E), Shear modulus (μ), and Poisson's ratio (σ) given by

$$E = 2\mu\,(1 + \sigma) \tag{10}$$

Uniaxial compressive strength UCS (for units of sand) was calculated from equation 11 by [25] given as:

$$UCS = 1200\exp^{(-0.036\Delta Tc)} \quad (11)$$

While UCS (for shale units) was calculated from equation 12 by [26] which is suitable for calculating UCS for high porosity Tertiary shales like those of the Niger Delta. It is given by

$$UCS = 10[\frac{304.8}{\Delta T_C^{-1}} \quad (12)$$

For the petrophysical parameters of the reservoirs, total porosity ($Ø_T$) was estimated from equation13 according to [27] given by:

$$Ø_T = \frac{(\rho_{ma} - \rho_b)}{(\rho_{ma} - \rho_{fl})} \quad (13)$$

Effective porosity ($Ø_{eff}$) was obtained by using the equation of volume of shale (equation 14) by [28] given as:

$$Ø_{eff} = \frac{(\rho_{ma} - \rho_b)}{(\rho_{ma} - \rho_{fl})} - \frac{V_{sh}(\rho_{ma} - \rho_{sh})}{(\rho_{ma} - \rho_{fl})} \quad (14)$$

where ρ_{ma} is the density of rock matrix (2.65g/cc); ρ_{fl} is the pore fluid density (1.1g/cc for water; 0.9g/cc for oil; and 0.74g/cc for gas); $\rho_{sh}$is the density of shale; and V_{sh} is the volume of shale.

Permeability was calculated using the porosity equation (equation 15) from [29] given by:

$$K = \frac{0.136Ø^{4.4}}{(S_{wirr})^2} \quad (15)$$

Ø represents effective porosity and S_{wirr} represents water saturation (irreducible).
S_{wirr} was calculated from equation 16 given as [29]

$$S_{wirr} = (\frac{F}{2000})^{1/2} \quad (16)$$

where F stands for formation factor calculated from F = a/m; a is the tortuosity factor given as 0.62; and m represents cementation factor given as 2.15.

Pore pressure and the principal stresses of total vertical stress, minimumand maximum horizontal stresses operating within the reservoirs were also determined using suitable empirical models.

Pore pressure (P_p) was calculated from equation 17 given as [30]:

$$P_p = \int_0^h \rho_f gh\, dh \quad (17)$$

where ρ_f is the pore fluid density; g is acceleration due to gravity; and h represents depth measured in feet.

Total vertical stress $S_v$was estimated in psi from equation 18 given as [31]:

$$S_v = \rho_b \times 1000 \times g \times h \times 0.3048 \times 0.000145037738 \quad (18)$$

Maximum horizontal stress $Sh_{max}$was obtained using the poroelastic model (equation 19) by [32] given by:

$$Sh_{max} = \frac{\sigma}{1-\sigma}(S_v - \alpha P_p) + \alpha P_p + \frac{E_{sta}}{1-\sigma^2}\mathcal{E}_y + \sigma\mathcal{E}_x \quad (19)$$

where α is the Biot constant, E_{sta} stands for static Young's modulus, $\mathcal{E}_x$and $\mathcal{E}_y$ represent strain at minimum and maximum horizontal directions of stress.

$\mathcal{E}_y$ and $\mathcal{E}_x$ were obtained from the following relationships (equations 20 and 21) by [33] given by:

$$\mathcal{E}_y = \frac{S_v\sigma}{E_{sta}}[\frac{1}{1-\sigma} - 1] \quad (20)$$

$$\mathcal{E}_x = \frac{S_v\sigma}{E_{sta}}[1 - \frac{\sigma^2}{1-\sigma}] \quad (21)$$

Static Young's modulus (E_{sta}) was calculated using the relationship (equation 22) by [34] given as:

$$E_{sta} = 0.731 \times E_{dyn} - 2.337 \quad (22)$$

The constants 2.337 and 0.731 are the Seyed and Aghighi numbers obtained from experiments performed using core samples in the laboratory.

Lastly, minimum horizontal stress (Sh_{min})was determined from the relation (equation 23) by [35] given by

$$Sh_{min} = \frac{\sigma}{1-\sigma}[S_v - \alpha P_p] + \alpha P_p \text{ in megapascals} \quad (23)$$

The Biot constant (α) was obtained using the [36] relation given in equation 24 as:

$$\alpha = 1 - K_b/K_r \qquad (24)$$

where K_b is the bulk modulus or incompressibility of the material; and K_r is the rock constituents bulk.

Core data was then used to validate the well log and seismic reflection information to ensure the units identified by well logs are correct and at the proper depths. Following this was a comparative analysis of the petrophysical and elastic reservoir properties with unconfined compressive strength (UCS) using cross plots. Ms-Excel was used in obtaining these cross plots. Finally, 3D geomechanical models for all the rock mechanical properties were then generated. The models are typically a distribution, in the spatiotemporal sense, of all the calculated rock mechanical parameters and they were generated through the horizontal extrapolation method. Stochastic methods were used in constructing the models while Variogram modeling and Sequential Gaussian modeling with collocated co-kriging computational procedure was also applied. A workflow showing the methodology employed for this study is shown in Figure 4.

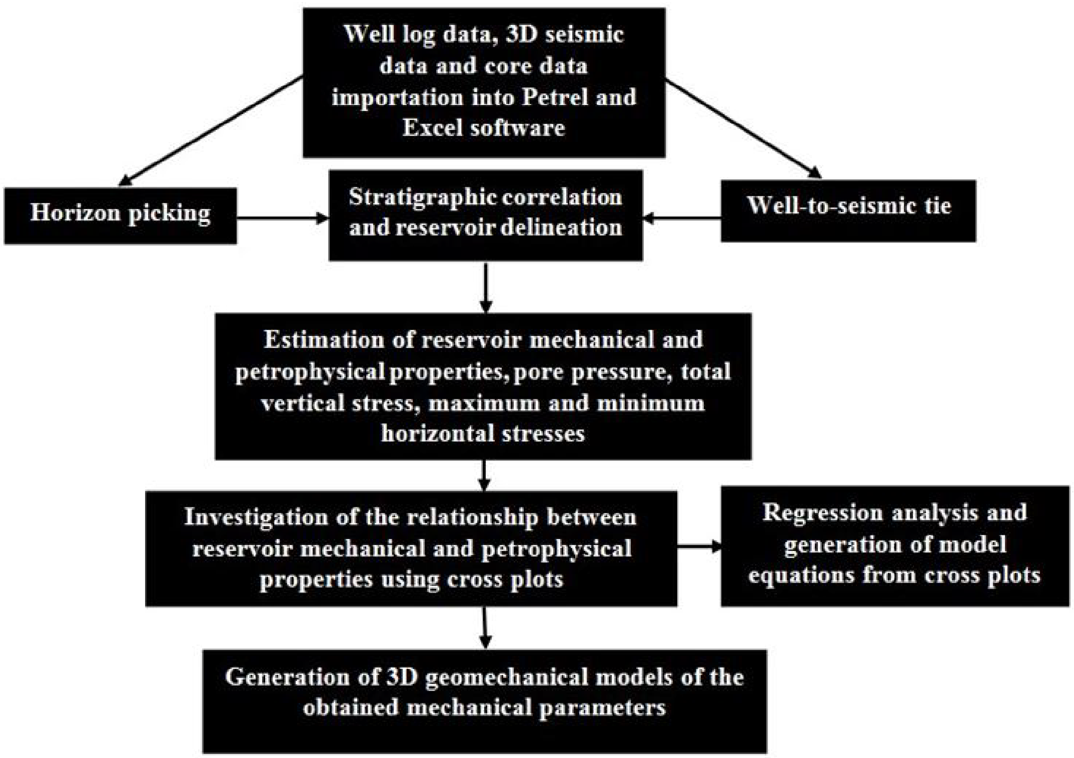

Figure 4. Workflow of the methodology employed in this study

4. Results and discussion

4.1. Reservoir delineation

Reservoir delineation was done using gamma ray logs by initially identifying surfaces of interest in Beta 1, Beta 2, Beta 3, and Beta 4 wells in a Well correlation panel. This fell between 8,860ft and 10,220ft in the central part of the field. Figure 5 shows the delineation and correlation of reservoirs for the four Beta wells using gamma ray logs.

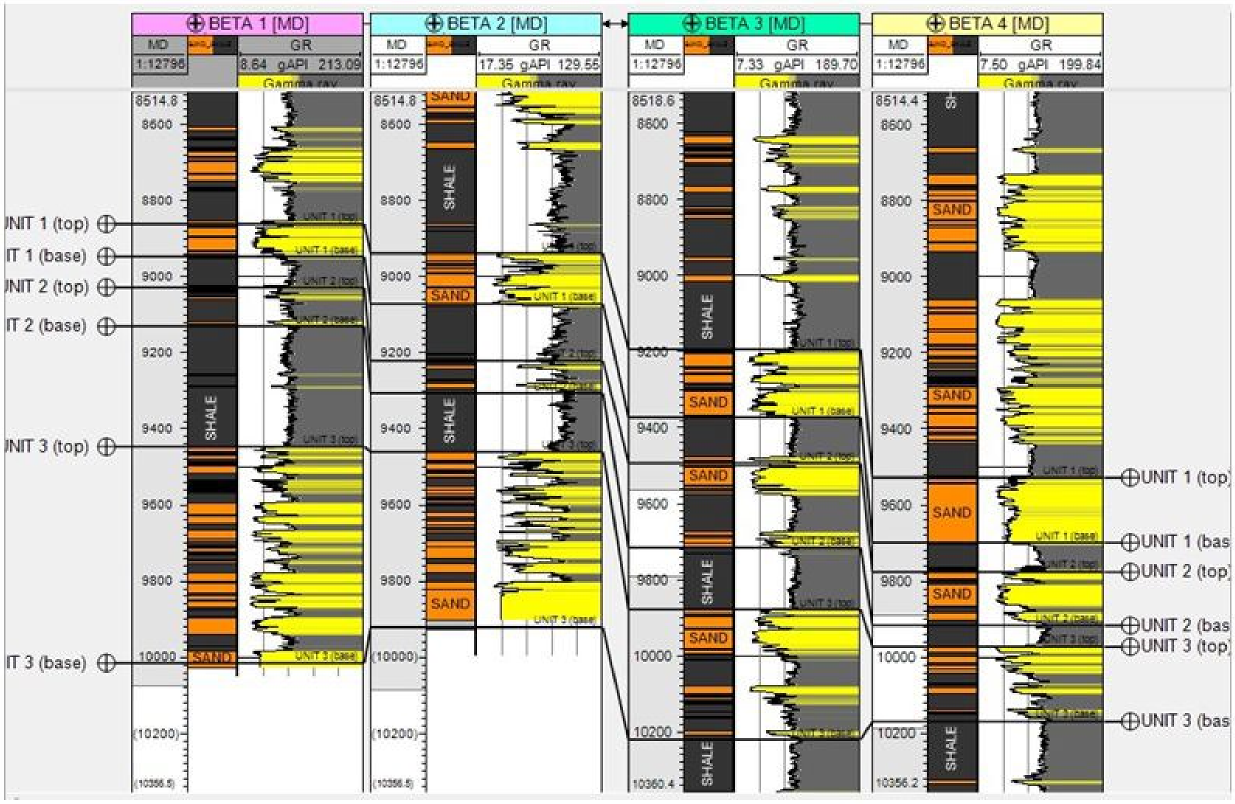

Figure 5. Delineation and correlation of reservoirs for Beta 1, Beta 2, Beta 3, and Beta 4 wells using gamma ray logs

4.2. Rock mechanical and petrophysical properties

The mechanical and petrophysical properties of the reservoirs were calculated using the empirical relationships in equations 1 to 16 as presented in the methodology section. The mean values of the rock mechanical and petrophysical properties, including Poisson's ratio, Young's modulus, bulk compressibility, bulk modulus, unconfined compressive strength, shear modulus, permeability, effective porosity, and total porosity for shale and sand units within Beta reservoirs are presented in Table 1.

Table 1. Mean values of the rock mechanical and petrophysical properties for sand and shale within the studied reservoirs

S/N	Property	Average for sand	Average for shale
1.0	Young's modulus	10.94±1.52 GPa	13.70±1.90 GPa
2.0	Bulk modulus	12.76±2.12 GPa	13.30±2.01 GPa
3.0	Shear modulus	4.11±1.03 GPa	5.12±1.27 GPa
4.0	Poisson's ratio	0.30±0.02	0.33±0.03
5.0	Bulk compressibility	0.10±0.03 GPa^{-1}	0.07±0.014 GPa^{-1}
6.0	UCS	25.19±14.15 GPa	32.32±17.52 GPa
7.0	Total porosity	0.25±0.07	0.09±0.02
8.0	Effective porosity	0.19±0.09	0.07±0.01
9.0	Permeability	192.00±53.9 mD	0.022±0.016 mD

The depth profiles of the mechanical and petrophysical parameters of the reservoir rock depicted by gamma ray, shear modulus, bulk modulus, Young's modulus, unconfined compressive strength, bulk compressibility, effective porosity, sonic, and total porosity for the four Beta Wells are shown in Figure 6a to 6d.

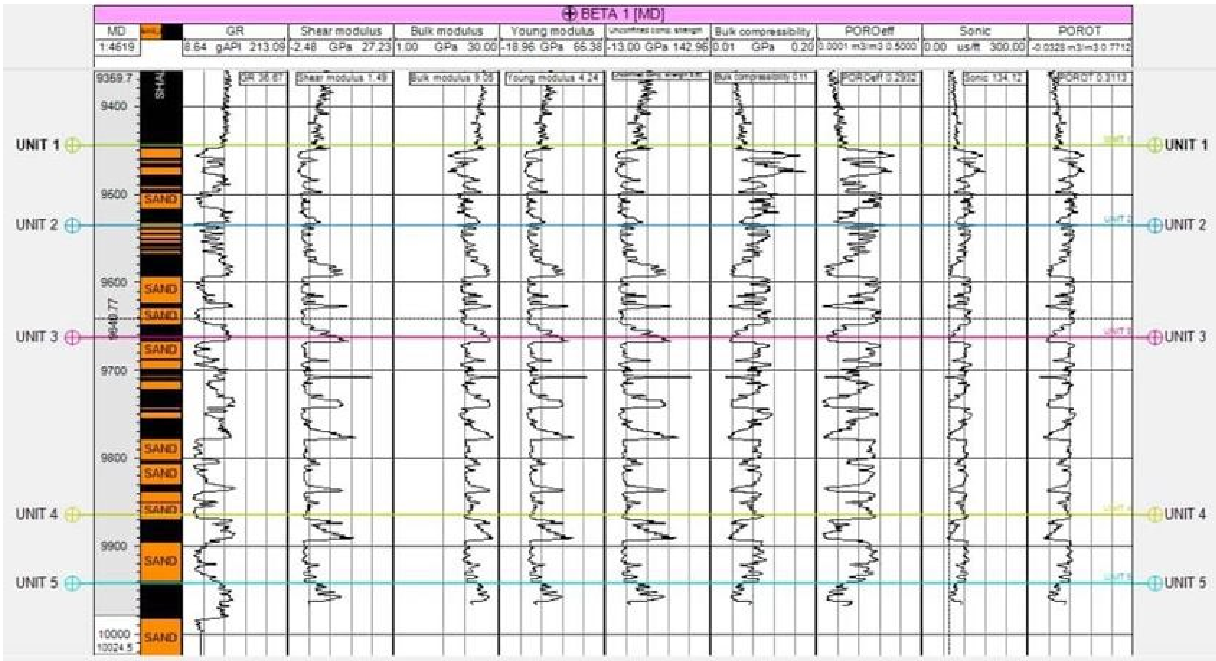

Figure 6a. Depth profiles of gamma ray, shear modulus, bulk modulus, Young's modulus, unconfined compressive strength, bulk compressibility, effective porosity, sonic, and total porosity in Beta 1 Well.

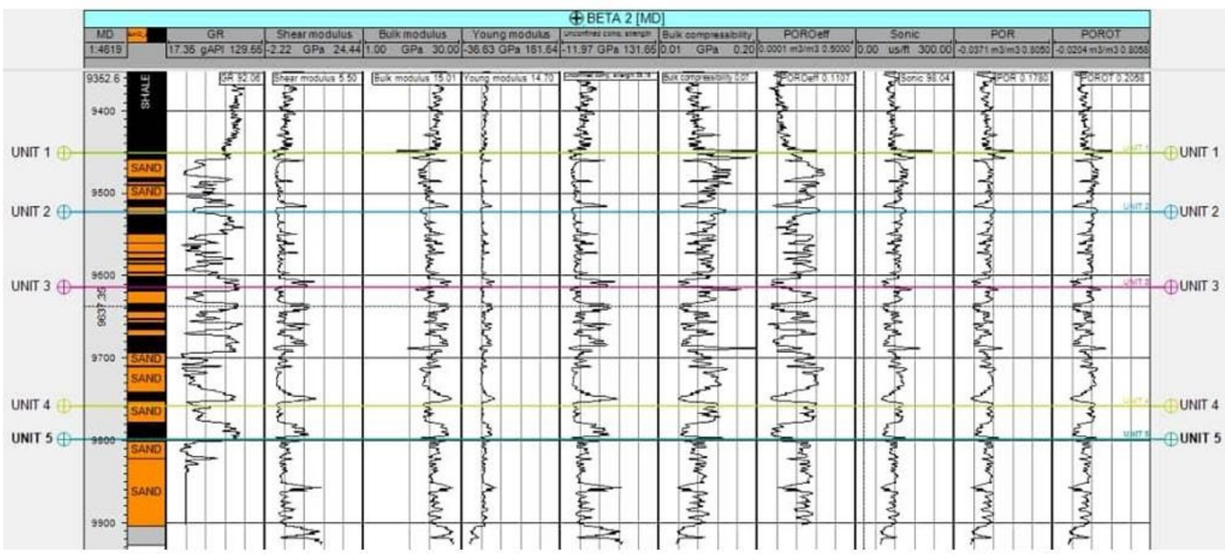

Figure 6b. Depth profiles of gamma ray, shear modulus, bulk modulus, Young's modulus, unconfined compressive strength, bulk compressibility, effective porosity, sonic, and total porosity in Beta 2 Well.

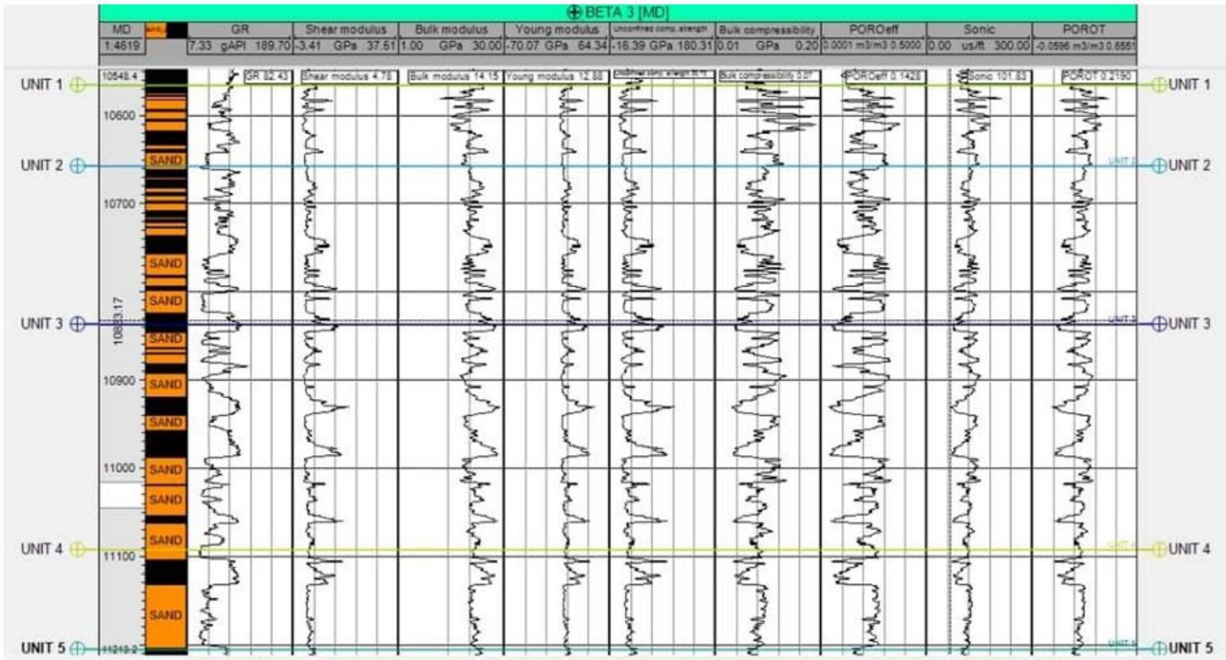

Figure 6c. Depth profiles of gamma ray, shear modulus, bulk modulus, Young's modulus, unconfined compressive strength, bulk compressibility, effective porosity, sonic, and total porosity in Beta 3 Well.

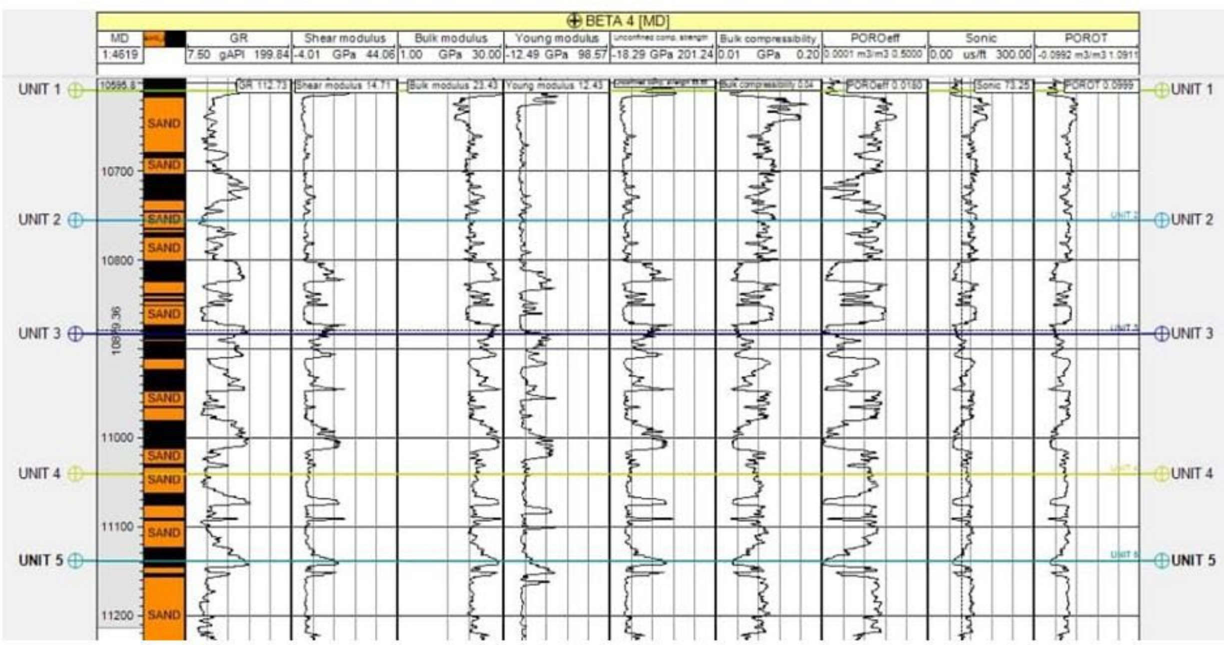

Figure 6d. Depth profiles of gamma ray, shear modulus, bulk modulus, Young's modulus, unconfined compressive strength, bulk compressibility, effective porosity, sonic, and total porosity in Beta 4 Well.

4.3. Principal stresses and pore pressure in the reservoirs

Total vertical stress, minimum and maximum stresses in the horizontal direction as well as pore pressure operating in the reservoirs were evaluated from the relationships in equations 17 to 24 presented in the methodology section. This was carried out to assess the level of stability of these reservoirs by comparing the estimated principal stresses and pore pressure with obtained mechanical parameters of the reservoirs. Mean values of these principal stresses and pore pressure are presented in Table 2.

Table 2. Calculated mean amounts of pore pressure (in sand and shale), total vertical stress, minimum horizontal stress and maximum horizontal stress in Beta reservoirs

Parameter	Minimum (psi)	Maximum (psi)	Average (psi)
Pore pressure (P_p) (Sand)	13,228.9	14,184.6	13,683±390.3
Pore pressure (P_p) (Shale)	15,111.6	16,015.0	15,662±279.5
Total vertical stress (S_v)	27,755.9	29,431.6	28,392±629.0
Maximum horizontal stress (Sh_{max})	24,671.9	26,161.4	25,537±440.6
Minimum horizontal stress (Sh_{min})	20,045.9	21,256.2	20,781±330.5

4.4. Cross-plots of mechanical and petrophysical rock properties

Existing interrelationship between rock elastic, inelastic, and petrophysical properties was investigated to verify the suggestion by [8] and [37] that there exists a connection between the elastic properties of rock, depth, and the rock compressive strength (UCS) of a reservoir. Figure 7a to 7d are cross-plots indicating the connection between some of these rock parameters.

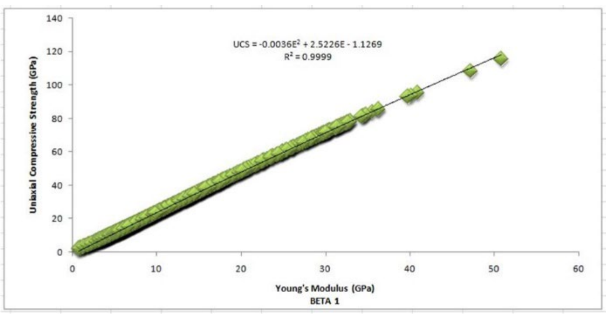

Fig. 7a. Cross-plot showing trend line of compressive rock strength against Young's modulus

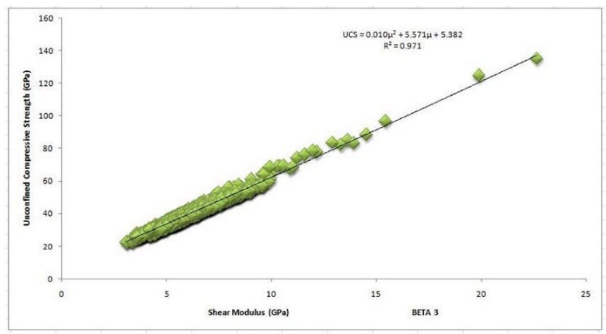

Fig. 7b. Cross-plot showing trend line of unconfined compressive strength against shear modulus

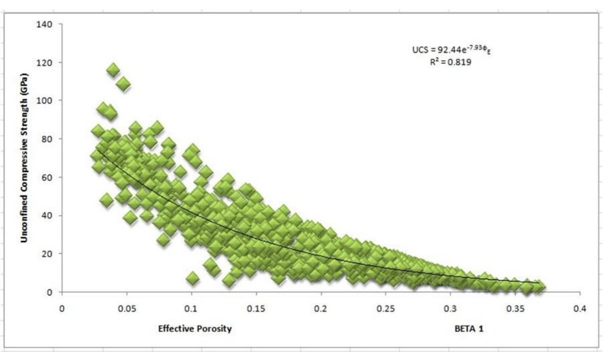

Fig. 7c. Cross-plot showing trend line of unconfined compressive strength against effective porosity

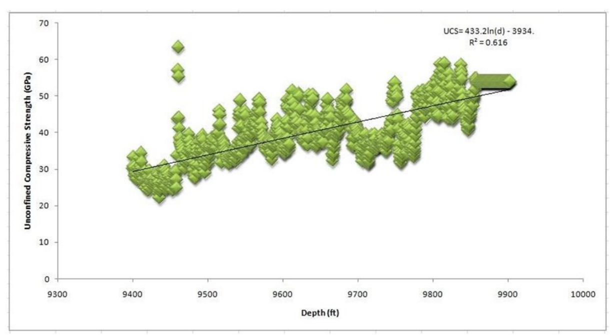

Fig. 7d. Cross-plot showing trend line of unconfined compressive strength against depth

From the obtained cross plots, four model equations were derived and established using regression analysis. In each case, linear, quadratic, power, logarithmic and exponential regression models were evaluated and their prediction performances were analyzed using statistical parameters including the sum of squares error (SSE), the sum of squares regression (SSR), the sum of squares total (SST) and coefficient of determination (R-Squared). The quadratic regression model gave the most R-squared value for UCS versus Young's modulus (99%) and UCS versus shear modulus (97%), exponential regression model gave the most R-squared value for UCS versus effective porosity (82%), while the logarithmic model gave the most for UCS versus depth (62%). The obtained model equations are shown in equations 25 to 28.

$$UCS = -0.0036E^2 + 2.5226E - 1.1269 \quad (25)$$

where UCS = unconfined compressive strength and E = Young's modulus in Gigapascal (GPa).

$$UCS = 0.010\mu^2 + 5.571\mu + 5.382 \quad (26)$$

where μ = shear modulus in gigapascal (GPa).

$$UCS = 92.44e^{-7.93\phi_E} \quad (27)$$

where ϕ_E = effective porosity

$$UCS = 433.2\ln(d) - 3934 \quad (28)$$

where d = measured depth in feet (ft).

4.5. Geomechanical models

3D mechanical earth models representing spatial distribution of mechanical properties of the studied reservoir rock were generated and variations in the elastic properties and rock strength across the reservoir top were identified. The models generated include Young's modulus model, Poisson's ratio model, shear modulus model, bulk modulus model, bulk compressibility model, and compressive rock strength model. Figure 8a to 8f shows the generated geomechanical earth models.

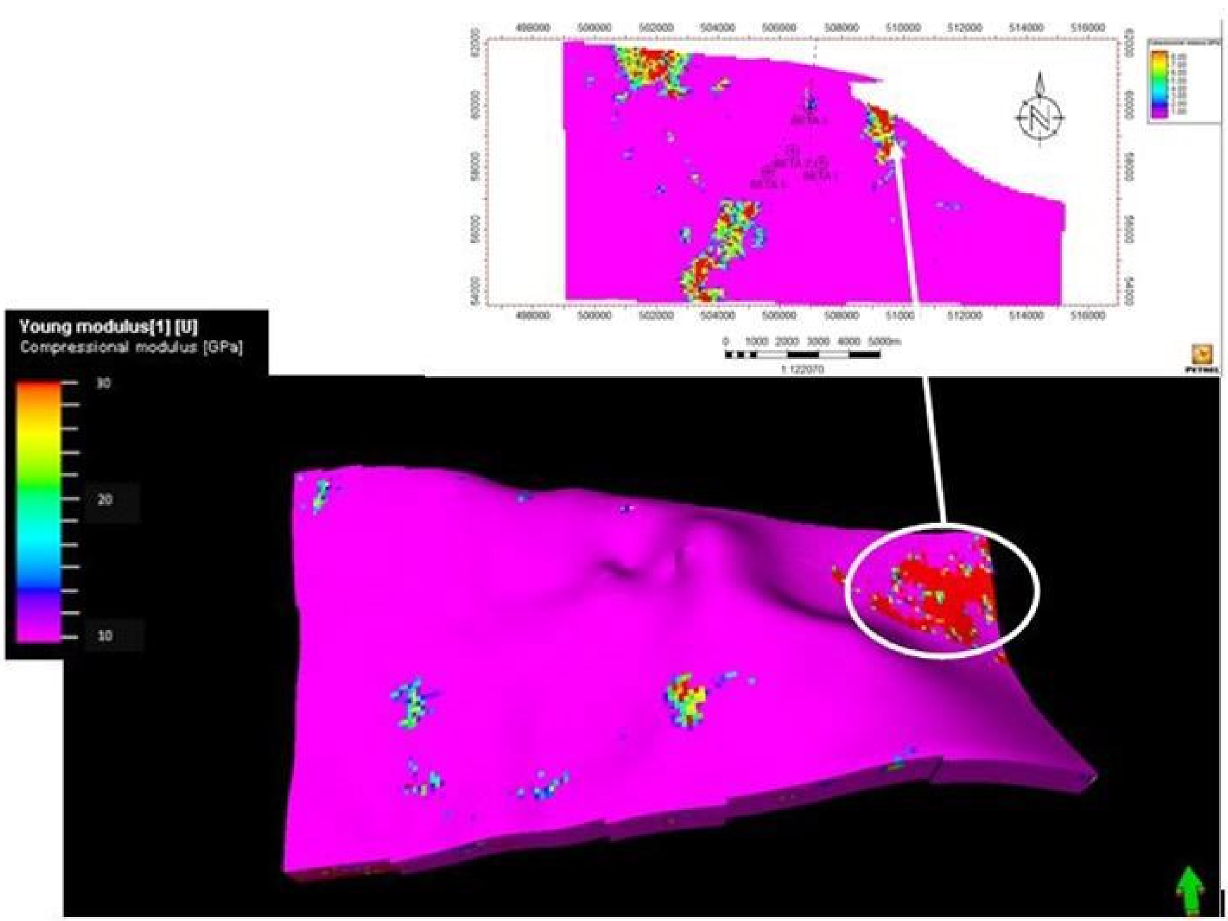

Figure 8a. 3D mechanical earth model with an inserted map indicating lateral distribution of Young's modulus across the reservoir top

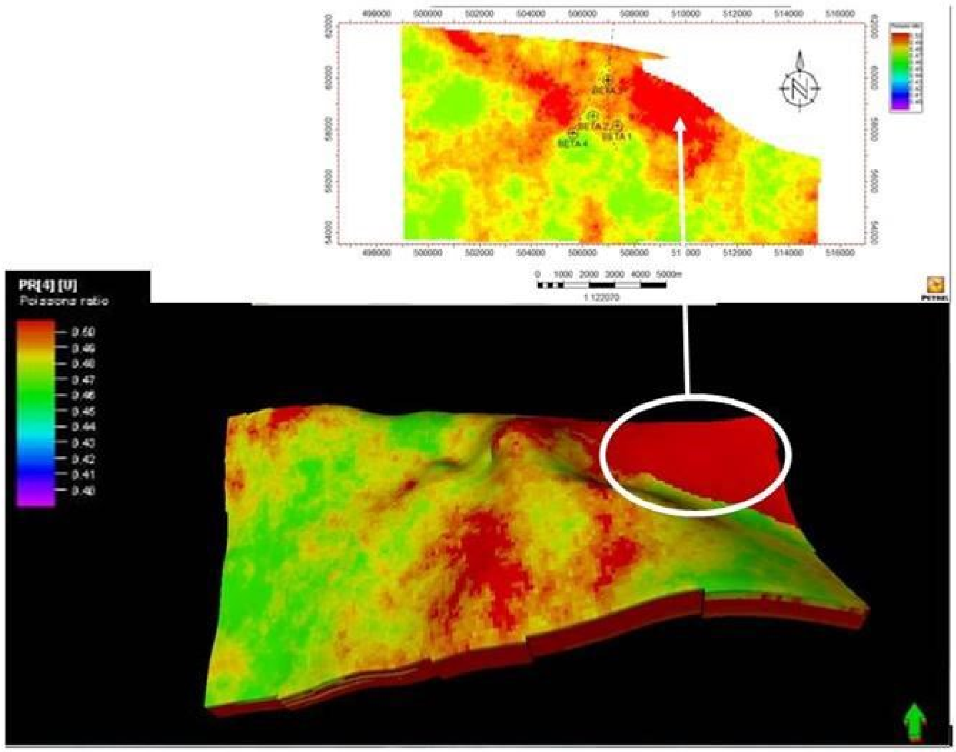

Figure 8b. 3D mechanical earth model with an inserted map indicating lateral distribution of Poisson's ratio across the reservoir top.

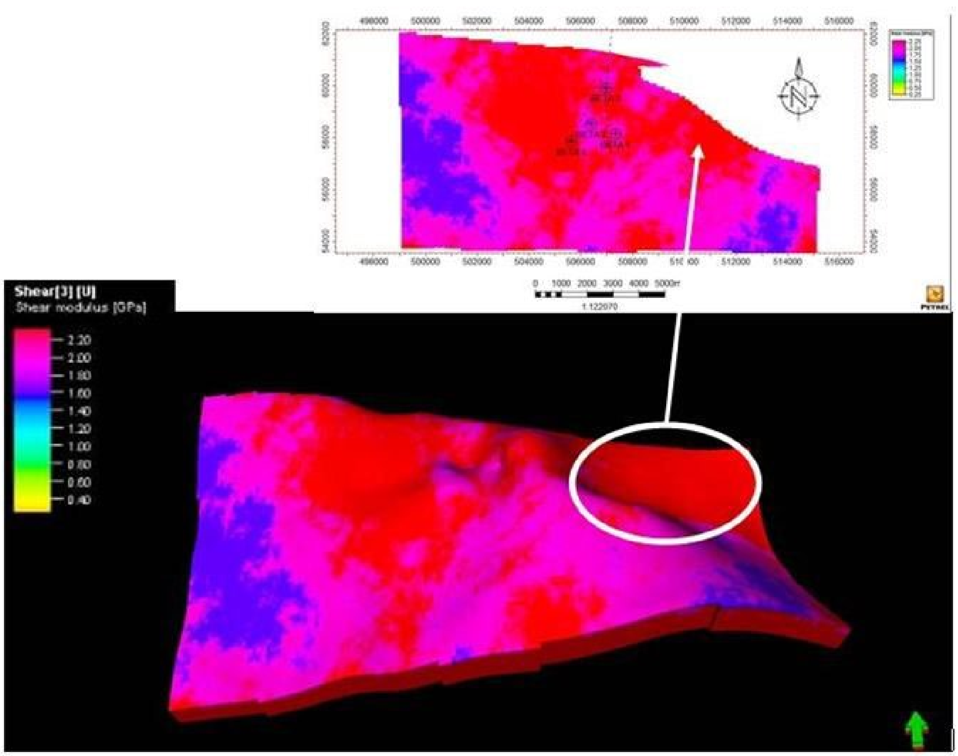

Figure 8c. 3D mechanical earth model with an inserted map indicating lateral distribution of shear modulus across the reservoir top.

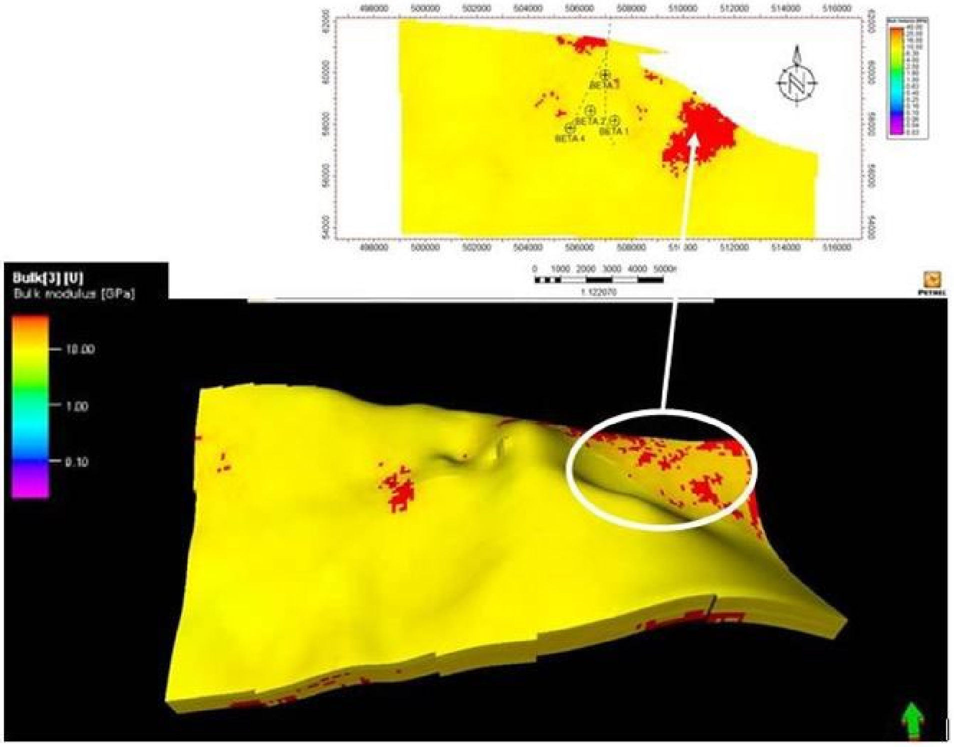

Figure 8d. 3D mechanical earth model with an inserted map indicating lateral distribution of bulk modulus across the reservoir top.

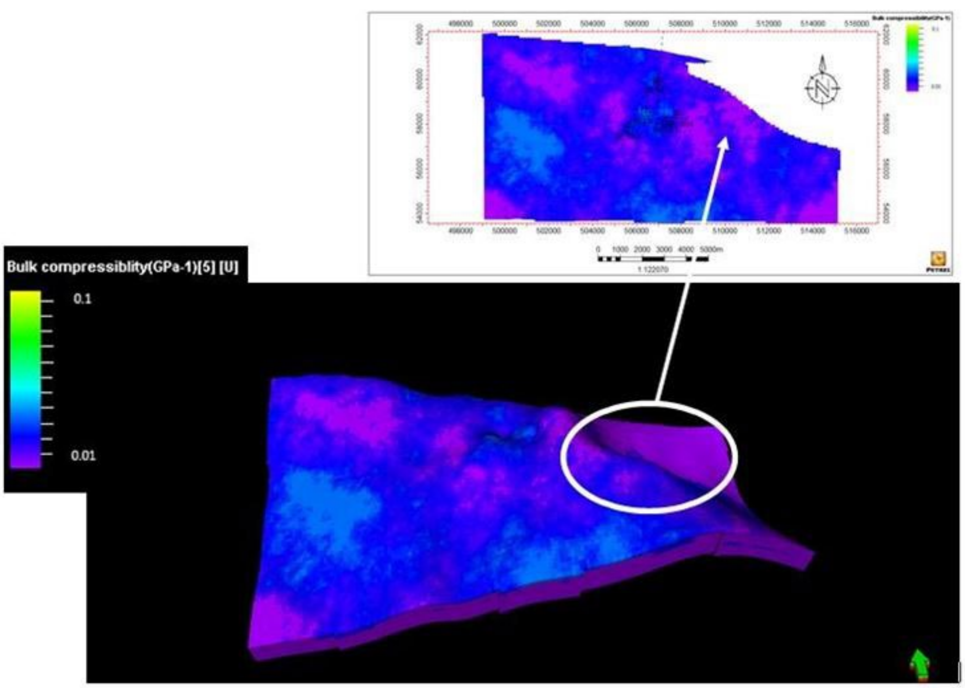

Figure 8e. 3D mechanical earth model with an inserted map indicating lateral distribution of bulk compressibility across the reservoir top.

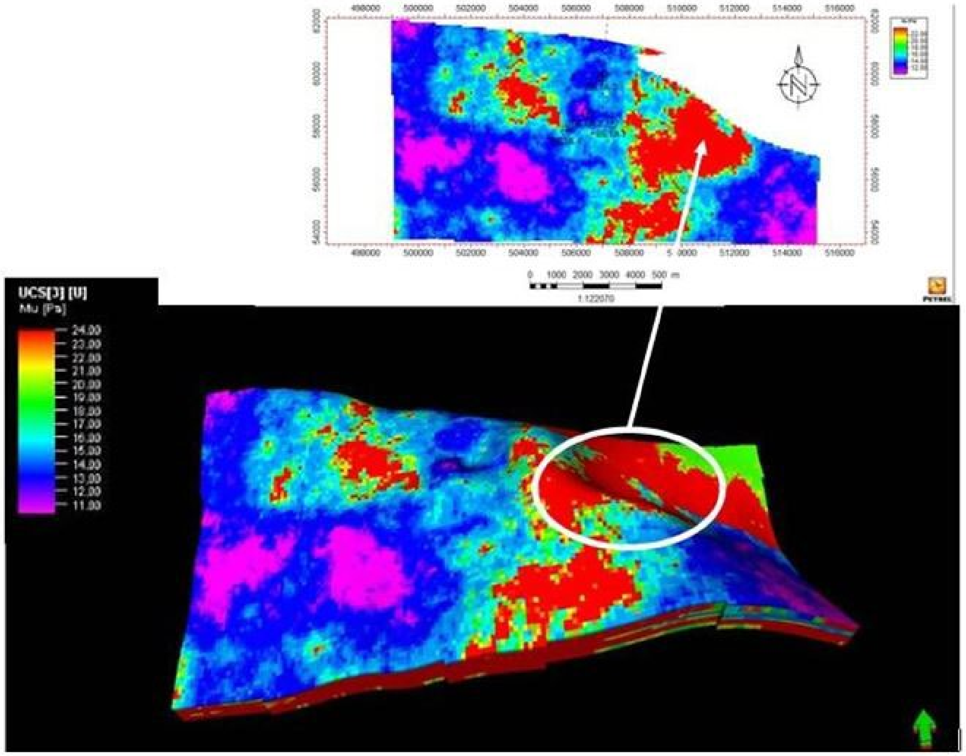

Figure 8f. 3D mechanical earth model with an inserted map indicating lateral distribution of unconfined compressive strength across the reservoir top

From results of reservoir delineation using well log data, the reservoirs range in the interval from a depth of 8,860ft to a depth of 10,220ft. The lithological and stratigraphic investigation of the reservoirs reveals that the geological units are mainly sand and shale as can be seen in Figure 5. The reservoir lithology shows a sand sequence with shale intercalations (paralic) and the depth describes a formation with shale and sand units deposited in almost equal proportion with the sand unconsolidated. According to [16], this validates the formation to be the Niger Delta Agbada Formation.

Results of the evaluation of reservoir rock dynamic mechanical and petrophysical properties show a noticeable change in the mean values of these properties between sand and shale within the extent of the reservoirs. While the mean rates of the mechanical parameters are greater in shale units, the mean rates of the petrophysical parameters are greater in sand units as presented in Table 1. This implies that the shale units are stronger and more competent than the sand units and is an indication that the sand of the studied reservoir will more rapidly deform or even fail than the shale under the same stress conditions while the shale will very likely form a seal to the fracture growth [11].

Results of pore pressure analysis indicate a higher pore pressure in shale units compared to sand units. The pore pressure in shale falls within the overpressure regime, with pressures approaching 16,000psi. This is chiefly a result of disequilibrium compaction and other fundamental reasons [38]. The magnitudes of the principal stresses observed within the reservoirs are such that the minimum horizontal stress is the least. This is followed by the maximum horizontal stress which is less than the recorded total vertical stress ($Sh_{min}<Sh_{max}<S_v$). The overall implication of this is the existence of a normal fault stress system in this field and associated petroleum plays [12]. Shear failure will very likely be the failure mechanism in this field as a result of the high differential stress recorded [39]. Also, analyses of these stresses have revalidated the existence of active faults and tectonic operations within the Niger Delta. This is due to the difference in magnitude observed between the two principal horizontal stresses (Sh_{min} and Sh_{max}). Comparative analysis of the magnitudes of these principal stresses

operating within the reservoirs and the magnitudes of the obtained mechanical properties of the reservoirs show that these reservoirs are very stable and are not under increased risk of deformation or failure during exploration, exploitation, or enhanced oil recovery processes.

From the cross-plots of the inelastic, elastic, and petrophysical parameters of the reservoir rock, there is a conspicuous connection between these rock properties as can be seen in Figure 7a to 7d. There is a clear increase in compressive rock strength with elastic properties of shear modulus and Young's modulus as well as with depth. This indicates that increasing values of the elastic rock parameters and the rock's depth of burial leads to an increase in the rock strength. The elasticity and compaction of a unit of rock determines to a large extent the ductility and strength of that rock. Also, there is a decrease in compressive rock strength and by extension the rock elastic parameters with porosity. This shows that the presence of pore spaces within a rock unit decreases the overall strength of that rock and makes the rock highly susceptible to deformation when subjected to stress. A highly porous rock unit will yield rapidly to deformation than a less porous rock when exposed to the same stress conditions

Considering the generated 3D geomechanical models of the studied reservoirs, it can be observed from the inserted legends that the reservoir rock mechanical and strength properties have increased values in the North-northeastern (NNE) portion of the field. The direct implication of this is that mechanical rock deformation and possible failure during Well drilling, exploitation, and enhanced oil recovery techniques like hydraulic fracturing will be low in this section of the field compared to other sections with low mechanical properties.

4.6. Discussion

It is observed from this study that the maximum horizontal stress in this field is greater than the minimum horizontal stress which is less than the total vertical stress. This result is in agreement with the findings of [12] in their evaluation of the geomechanical characteristics of an oilfield in the onshore Niger Delta. This shows that the Niger Delta is characterized by normal fault stress system. One of the key findings of this study is also in agreement with the result obtained by [40] in his geomechanical and petrophysical characterization of the reservoir of Wabi Field in the north-central axis of the Niger Delta. He compared estimated geomechanical parameters with in-situ stresses within the environment and observed that the reservoirs are stable.

The relationship between rock mechanical and petrophysical properties for sand and shale observed in this study show strong similarity with the findings of [41] in their study of the relationship between physical properties and rock strength in sedimentary rocks. They carried out comparisons of various empirical relations to determine the dependence of UCS of sandstone and shale on compressional wave velocity (Vp), Young's modulus, and porosity and noticed an increase in Young's modulus and Vp with UCS but a decrease in UCS with increasing porosity which is similar to what is obtained in this study. In a similar study conducted for massive to medium to thickly bedded, red, coarse-grained, and pebbly volcanic sandstone, and massive, unbedded, poorly sorted, lapilli tuff and matrix-to-clast-supported coarse breccias belonging to Borrowdale Volcanic Group, Sellafield, [42] obtained a result which agrees with the result of this study. They observed that UCS increased exponentially with sonic velocity but decreased exponentially with increasing effective porosity, while sonic velocity decreased with increasing effective porosity. The same can also be said of the results obtained by [8] in the estimation of geomechanical parameters of North Sea shale from empirical relations. From his findings, shear modulus, Young's modulus, and UCS increased with increasing Vp while UCS decreased with increasing total porosity which is in agreement with results of this study.

In this study, the 3D earth models generated revealed areas of mechanical rock weakness which will control the setting up of future exploratory wells in the field. This is in agreement with the results put forward by [10] that revealed high and low risk areas of mechanical rock deformation in a reservoir through 3D earth modeling as well as reservoir modeling, offshore Brazil.

Another study carried out to determine the geomechanical parameters of rocks of hydrocarbon reservoirs in the onshore Niger Delta by [5] revealed mean values of 0.28, 2.4GPa, 10.5GPa, 6.83GPa, and 14.44MPa for sand and 0.35, 8.93GPa, 18.08GPa, 21.01GPa, and 56.17MPa for shale respectively representing Poisson ratio, Young, Bulk, Shear modulus, and UCS. This implies superiority in the strength and ductility of the reservoir shale over sand in that field which also agrees totally with the results of this study.

5. Conclusion and recommendation

The mechanical attributes of the reservoir rocks of Beta Field in the offshore depobelt of the Niger Delta have been carefully studied and geomechanical models generated by leveraging on an integrated approach involving well log information, core information, and seismic 3D volume from the field. Results of this study have clearly shown that rock mechanical properties are central and critical in determining the success or otherwise of hydrocarbon exploration and exploitation activities. It can therefore be concluded from the findings of this study that the integration of well log information, seismic 3D information, and information from core samples provide very detailed geomechanical information that is invaluable in mitigating geomechanical-related exploration and exploitation problems often encountered by operators in the field. The 3D seismic volume and petrophysical information help in analyzing the spatial variation of rock elastic moduli and strength even for undrilled sections of the reservoir. This information is critical in reducing the risks associated with the geomechanical problems while increasing overall productivity. It can also be concluded that the reservoirs of this field are significantly stable.

Based on the findings of this study, it is recommended that adequate care should be taken when placing future exploratory wells in the portions of this field with low mechanical and rock strength parameters. Adequate pressure management should be applied to prevent drilling and exploitation challenges. This will contribute in no small way in preventing the myriad of problems usually faced by operators throughout the useful life of a field, particularly in unconventional environments.

It is also recommended that the obtained model equations should be utilized in the estimation of UCS from any of Young's modulus, shear modulus, effective porosity, and measured depth for offshore Niger Delta and similar geologic terrains without facing the operational challenges involved in going to the field for such measurements.

Conflict of interest

The authors have no relevant financial or non-financial interests to disclose.

Acknowledgment

The authors are grateful to the management of BGP/CNPC for providing the necessary data, workstation, and software needed to carry out this study.

References

[1] Mehrdad S. Application of Geophysical Data for Geomechanical Studies: A Critical Review, PetroGem Incorporated, 2015.

[2] McPhee C, Reed J, Zubizarreta I. Core Analysis: A Best Practice Guide. Developments in Petroleum Science, Elsevier, 2015; 64(1): 2-829.

[3] Whaley J. An Introduction to Geomechanics. Geoscience Magazine, 2019; 6(2).

[4] Abedifar M, and Abedideh M. A sensitivity study of geomechanical and reservoir parameters on safe mud window during drilling operations. Pet Coal, 2017; 59(4): 489-496,

[5] Osaki LJ, Uko ED, Iyeneomie TA, Alabraba MA. Geomechanical Characterization of a Reservoir in Part of the Niger Delta, Nigeria. Asian Journal of Applied Science and Technology, 2019; 3(1): 10-30.

[6] Qiuguo L, Zhang X, Al-Ghammari K, Mohsin L, Jiroudi F, Al-Rawahi A. 3D Geomechanical Modeling, Wellbore Stability Analysis Improve Field’s Performance. World Oil journal published by Gulf Publishing Company, 2013; 53-61.

[7] Fredrich JT, Arguello JG, Deitrick GL. Geomechanical Modeling of Reservoir Compaction, Surface Subsidence, and Casing Damage at the Belridge Diatomite Field, California. Society of Petroleum Engineers, 2000; 3, ID: SPE-65354-PA, DOI: https://doi.org/10.2118/65354-PA.

[8] Horsrud P. Estimating Mechanical Properties of Shale from Empirical Correlations." SPE Drilling and Completion, 2001; 16(2): 68–73.

[9] Nygaard R. Geomechanical Analysis of Wabamun Area Carbon Dioxide Sequestration Project (WASP). Energy and Environmental Systems Group, Institute for Sustainable Energy, Environment and Economy (ISEEE), University of Calgary, Colombia, 2010.

[10] De Souza ALS, De Souza JAB, Meurer GB, Naveira VP, Chaves RAP, Frydman M, Pastor J. Integrated 3D Geomechanics and Reservoir Simulation; Optimize Performance, Avoid Fault Reactivation. World Oil journal, 2014; 55-58.

[11] Agoha CC, Opara AI, Okeke OC, Okereke CN, Onwubuariri CN, Akiang FB, Osaki LJ, Omenikolo IA. Integrated 3Dgeomechanical characterization of a reservoir: case study of "Fuja" field, offshore Niger Delta, Southern Nigeria. Journal of Petroleum Exploration and Production Technology, 2021; 11: 3637–3662, https://doi.org/10.1007/s13202-021-01244-9.

[12] Abijah FA, Tse AC. Geomechanical Evaluation of an Onshore Oil Field in the Niger Delta,Nigeria. IOSR Journal of Applied Geology and Geophysics, 2016; 4(1): 99-111.

[13] Osaki LJ, Uko ED, Opara AI. 3D Geomechanical Reservoir Model for Appraisal and Development of Emi-003 Field in Niger Delta, Nigeria. Asian Journal of Applied Science and Technology, 2018; 2(4): 276-294.

[14] Zoback MD. Stress-Field Constraints on Intraplate Seismicity in Eastern North American. Journal of Geophysical Research-Solid Earth, 1992; 97, B8, 11761-11782.

[15] Nton ME, Esan TB. Sequence Stratigraphy of EMI Field, Offshore Eastern Niger Delta, Nigeria. European Journal of Scientific Research, 2010; 44 (1): 115-132.

[16] Doust H, Omatsola E. Niger Delta, in Edwards, J. D., and Santogrossi, P. A., eds., Divergent/passive Margin Basins, AAPG Memoir 48: Tulsa, American Association of Petroleum Geologists, 1990; 239-248.

[17] Short KC, Stauble AJ. Outline of Geology of Niger Delta. The American Association of Petroleum Geologists Bulletin, 1967; 51(5): 761-779.

[18] Evamy BD, Harembourne J, Kamerling P, Knaap WA, Molley FA, Rowlands PH. Hydrocarbon habitat of the Tertiary Niger Delta; AAPG bulletin, 1978; 62: 1–39.

[19] Reyment RA. Aspects of the Geology of Nigeria. University of Ibadan Press Ibadan Nigeria, 1965.

[20] Weber KJ, Daukoru EM. Petroleum Geology of the Niger Delta: Proceedings of the ninth World Petroleum Congress, 2, Geology: London, Applied Science Publishers, Ltd., 1975; 210-221.

[21] Whiteman AJ. Nigeria: Its Petroleum Geology, Resources, and Potential, 1 and 2, Graham and Trottan, London, 1982; 394.

[22] Opara AI, Onuoha KM, Anowai C, Onu NN, Mbah RO. Geopressure and Trap Integrity Predictions from 3D Seismic Data: Case Study of the Greater Ughelli Depobelt, Niger Delta. Oil and Gas Science and Technology – Rev. IFP Energies Nouvelles, 2012.

[23] Sheriff RE. Encyclopedic Dictionary of Exploration Geophysics (4th ed.). Society of Exploration Geophysicists, SEG Geophysical Reference Series, 2002; 13. http://dx.doi.org/10.1190/1.9781560802969.

[24] Greenberg ML, Castagna JP. Shear wave velocity estimation in porous rocks: theoretical formulation, preliminary verification and applications 1. Geophysical Prospecting, 1992; 40(2): 195–209. https://doi.org/10.1111/j.1365-2478.1992.tb00371.x.

[25] McNally GH. Estimation of coal measures rock strength using sonic and neutron logs. Geoexploration, 1987; (24): 381 – 395.

[26] Lal M. Shale Stability: Drilling Fluid Interaction and Shale Strength. SPE Asia Pacific Oil and Gas Conference and Exhibition Paper, Jakarta, 1999; 20–22: SPE 54356. Lama, R. & Vutukuri, V. 1978.

[27] Schlumberger. Log Interpretation Principles/Application. Schlumberger Wireline and Testing, 1989; 51

[28] Asquith GB, Gibson CR. Basic Well Log Analysis for Geologists. The American Association of Petroleum Geologists (AAPG), Tulsa, 1982.

[29] Adiela UP, Ayodele M, Okafor CA. Petrophysical Attributes and Reservoir Productivity Index of Eta-1 Well, X-Field, Niger Delta, Nigeria. International Journal of Advance Research and Innovative Ideas in Education, 2017; 3(4): 3292-3304.

[30] Jones ME, Leddra MJ, Goldsmith AS, Edwards D. The Geomechanical Characteristics of Reservoirs and Reservoir Rocks. Health and Safety Executive - Offshore Technology Report. London: HMSO Books, 1992.

[31] Omar I. Reservoir geomechanics lecture slides. Stanford University, 2015; Available from: https://lagunita.Stanford.edu./Course v1…about.
[32] Ostadhassan M, Zong Z, Zamrian S. Geomechanical modeling of an anisotropic formation Bakken: Case study. 46th US Rock, 148 Mechanics/Geomechanics Symposium, American Rock Mechanics Association, 2012.
[33] Kidambi T, Kumar GS. Mechanical earth modeling for a vertical well drilled in a naturally fractured light carbonate gas reservoir in the Persian Gulf. Journal of Petro. Sci. Eng., 2016; 141: 38-51.
[34] Seyed SS, Aghighi MA. Building and analyzing geomechanical model of Bangestan reservoir in Kopal oil field, Iranian. Journal of Mining Engineering, 2015; 10: 21-34.
[35] Ahmed U, Markley ME, Crary SF. Enhanced in-situ stress profiling with microfracture, core, and sonic logging data. SPE Form. Eval., 1991; 6(02): 243-251.
[36] Schlumberger. Well Evaluation Conference. Nigeria, 1985.
[37] Wong TF, David C. The transition from brittle faulting to cataclastic flow in porous sandstones: Mechanical deformation. Journal of Geophysical Research, 1997; 102 (B2): 3009–3025.
[38] Opara AI. Origin and generation mechanisms of geopressures in shale-dominated settings worldwide: a review. Global journal of pure and applied sciences, 2010; 16(4): 429-438.
[39] Wilson G, Cosgrove JW. Introduction to small-scale geological structures. George Allen and Unwin Publishers Ltd, 1982.
[40] Zorasi CB. Petrophysical and Geomechanical Characterization of a Marginal (Wabi) Field Reservoir in North-Central Niger Delta. Robert Gordon University [online], MRes thesis, 2019; Available from: https://openair.rgu.ac.uk.
[41] Chang C, Zoback MD, Khaksar A. Empirical relations between rock strength and physical properties in sedimentary rocks. Journal of Petroleum Science and Engineering, 2006; 51: 223–237.
[42] Entwisle DC, Hobbs PRN, Jones LD, Gunn D, Raines MG. The relationships between effective porosity, uniaxial compressive strength, and sonic velocity of intact Borrowdale Volcanic Group core samples from Sellafield. British Geological Survey, Keyworth, Nottingham NG12 5GG, 2005; https://doi.org/10.1007/s10706-004-2143-x

To whom correspondence should be addressed: Dr. C. C. Agoha, Department of Geology, Federal University of Technology, P.M.B. 1526, Owerri, Imo State, Nigeria, E-mail: fadig24@yahoo.co.uk
Orcid: *0000000295131358*